Elsevier Editorial System(tm) for BBA - Molecular Basis of Disease

Manuscript Draft

Manuscript Number: BBADIS-15-311R1

Title: TARGETING THE INTERFACE OF THE PATHOLOGICAL COMPLEX OF α-SYNUCLEIN AND TPPP/p25

Article Type: Regular Paper

Keywords: α-synuclein, binding motives, neomorphic moonlighting function, TPPP/p25, Parkinson's disease

Corresponding Author: Prof. Judit Ovádi,

Corresponding Author's Institution: Institute of Enzymology, Research Centre for Natural Sciences, Hungarian Academy of Sciences

First Author: Sándor Szunyogh

Order of Authors: Sándor Szunyogh; Judit Oláh; Tibor Szénási; Adél Szabó; Judit Ovádi

Abstract: The pathological interaction of intrinsically disordered proteins, such as α-synuclein (SYN) and Tubulin Polymerization Promoting Protein (TPPP/p25), is often associated with neurodegenerative disorders. These hallmark proteins are co-enriched and co-localized in brain inclusions of Parkinson's disease and other synucleinopathies; yet, their successful targeting does not provide adequate effect due to their multiple functions. Here we characterized the interactions of the human recombinant wild type SYN, its truncated forms (SYN1-120, SYN95-140), a synthetized peptide (SYN126-140) and a proteolytic fragment (SYN103-140) with TPPP/p25 to identify the SYN segment involved in the interaction. The binding of SYN103-140 to TPPP/p25 detected by ELISA suggested the involvement of a segment within the C-terminal of SYN. The studies performed with ELISA, Microscale Thermophoresis and affinity chromatography proved that SYN95-140 and SYN126-140 - in contrast to SYN1-120 - displayed significant binding to TPPP/p25. Fluorescence assay with ANS, a molten globule indicator, showed that SYN, but not SYN1-120 abolished the zinc-induced local folding of both the full length as well as the N- and C-terminal-free (core) TPPP/p25; SYN95-140 and SYN126-140 were effective as well. The aggregation-prone properties of the SYN species with full length or core TPPP/p25 visualized by immunofluorescent microscopy demonstrated that SYN95-140 and SYN126-140, but not SYN1-120, induced co-enrichment and massive intracellular aggregation after their premixing and uptake from the medium. These data with their innovative impact could contribute to development of anti-Parkinson drugs with unique specificity by targeting the interface of the pathological TPPP/p25-SYN complex.

Response to Reviewers: Please, see the attached file (Szunyogh_etal_reply.docx), because it involves a figure.

*Highlights (for review)

- TPPP/p25 and α-synuclein (SYN) display physiological and pathological functions.
- Mutants/fragments of SYN were produced to identify the interface of TPPP/p25-SYN complex.
- 121-140 aa segment of SYN is crucial for TPPP/p25 binding.
- Targeting interface of proteins with multiple functions is an innovative strategy for drug discovery.

TARGETING THE INTERFACE OF THE PATHOLOGICAL COMPLEX OF α-SYNUCLEIN AND TPPP/p25

Sándor Szunyogh, Judit Oláh, Tibor Szénási, Adél Szabó, Judit Ovádi[§]

Institute of Enzymology, Research Centre for Natural Sciences, Hungarian Academy of Sciences, 1117 Budapest, Hungary

[§] Address correspondence to: Judit Ovádi, Institute of Enzymology, Research Centre for Natural Sciences, Hungarian Academy of Sciences, Budapest, Magyar tudósok körútja 2., H-1117, Hungary, Tel. (36-1) 3826-714; E-mail: ovadi.judit@ttk.mta.hu

E-mail addresses:

SSZ: szunyogh.sandor@ttk.mta.hu;

J. Oláh: olah.judit@ttk.mta.hu;

TSZ: szenasi.tibor@ttk.mta.hu;

ASZ: szabo.adel@ttk.mta.hu;

J. Ovádi: ovadi.judit@ttk.mta.hu

ABSTRACT

The pathological interaction of intrinsically disordered proteins, such as α-synuclein (SYN) and Tubulin Polymerization Promoting Protein (TPPP/p25), is often associated with neurodegenerative disorders. These hallmark proteins are co-enriched and co-localized in brain inclusions of Parkinson's disease and other synucleinopathies; yet, their successful targeting does not provide adequate effect due to their multiple functions. Here we characterized the interactions of the human recombinant wild type SYN, its truncated forms (SYN^{1-120}, SYN^{95-140}**),** a synthetized peptide ($SYN^{126-140}$) and a proteolytic fragment ($SYN^{103-140}$) with TPPP/p25 to identify the SYN segment involved in the interaction. The binding of $SYN^{103-140}$ to TPPP/p25 detected by ELISA suggested the involvement of a segment within the C-terminal of SYN. The studies performed with ELISA, Microscale Thermophoresis and affinity chromatography proved that SYN^{95-140} and $SYN^{126-140}$ - in contrast to SYN^{1-120} - displayed significant binding to TPPP/p25. Fluorescence assay with ANS, a *molten globule* indicator, showed that SYN, but not SYN^{1-120} abolished the zinc-induced local folding of both the full length as well as the N- and C-terminal-free (core) TPPP/p25; SYN^{95-140} and $SYN^{126-140}$ were effective as well. The aggregation-prone properties of the SYN species with full length or core TPPP/p25 visualized by immunofluorescent microscopy demonstrated that SYN^{95-140} and $SYN^{126-140}$, but not SYN^{1-120}, induced co-enrichment and massive intracellular aggregation after their premixing and uptake from the medium. These data with their innovative impact could contribute to development of anti-Parkinson drugs with unique specificity by targeting the interface of the pathological TPPP/p25-SYN complex.

KEYWORDS

α-synuclein, binding motives, neomorphic moonlighting function, TPPP/p25, Parkinson's disease

1. INTRODUCTION

The *intrinsically* disordered α-synuclein (SYN) and Tubulin Polymerization Promoting Protein/p25 (TPPP/p25) are extensively involved in the etiology of Parkinson's disease and other synucleinopathies [1-3]. Therapeutic targeting of these proteins by small molecules is a huge challenge because of their flexibility resulting in heterogeneous conformational states. In addition, these and many other disordered proteins display multiple, independent functions [1, 4-6]. The various functions of these moonlighting proteins are not coded at gene level, do not stem from genetic alterations, their functions are manifested themselves at protein level due to changes in cellular localization, cell type, their oligomeric state, and concentrations of substrates, cofactors or products [7]. A subclass of the moonlighting proteins are the neomorphic moonlighting proteins (NMPs), the physiological function of which can be converted into a pathological one mostly due to their hetero-associations with "pathological" partners distinct from the physiological ones [8, 9]. Thus, disordered proteins hallmarking conformational diseases are often belong to NMPs; the prototype of these proteins is the TPPP/p25. This finding lead us to the recognition that targeting the individual disordered proteins themselves does not seem to be a promising approach to the development of therapeutic treatments of Parkinson's disease.

TPPP/p25 is a brain-specific protein discovered in our laboratory as a tubulin binding protein, which modulates the dynamics and stability of the microtubule system by its bundling and acetylation-enhancing activities [10-12]. In normal brain, it plays a crucial role in the differentiation of the oligodendrocytes thus likely in the ensheathment of axons as well [13, 14]. In addition, TPPP/p25 is involved in the aggresome formation at the centrosome region, which functions as a cytoprotective mechanism by collecting the small toxic protein aggregates [11, 15]. The optimal intracellular expression of TPPP/p25 is a key factor in the physiology of the brain functions; either its lack or enrichment in oligodendrocytes leads to distinct CNS diseases: glioma and multiple system atrophy (MSA), respectively [2, 16]. The pathomechanism of these neurological disorders hallmarked by SYN and TPPP/p25 has not been clarified in details.

The central flexible CORE region of TPPP/p25 is likely responsible for the binding of SYN forming the pathological complex, but not for the binding with tubulin/microtubules forming the physiological one [17-19]. The structure of the disordered SYN has been characterized as well; it is constituted of 3 well-defined regions [20]. Two separate, non-interacting zinc binding sites have been identified within the SYN sequence, ^{50}H and ^{121}DNE^{123} at the N- and C-terminals, respectively [21]. Functionally, SYN stimulates the phosphorylation of tau, which could indirectly affect the stability of axonal microtubules. The involvement of the C-terminal 45 residues of SYN in its aggregation at extreme in vitro conditions was suggested; however, a 30-residue peptide was found to be ineffective as a competitor [22]. At physiological conditions, TPPP/p25 occurs in oligodendrocytes [13], while SYN is expressed in neurons [23, 24]; however, at pathological conditions these two proteins are enriched and co-localized in both cell types [2]. The mechanism of these processes is unknown; however, there are data that SYN could be taken up by cells from the medium, in

addition, it could be transported via exosomal cell-to-cell transmission [24-27]. Our recent data have shown that TPPP/p25 could also be taken up similarly to SYN [9]; moreover, it could be detected in the cerebrospinal fluid [28].

Recently we have characterized the interactions of TPPP/p25 with its physiological partners as well as with proteins hallmarking Parkinson's disease [9, 29]. The tight interaction of TPPP/p25 with SYN in vitro as well as its modest aggregation-promoting activity was also demonstrated in HeLa and CHO cells expressing TPPP/p25 ectopically [9]. In a recent paper, we have identified the TPPP/p25 segment involved in the contact surface at different organization levels using human recombinant wild type and mutant proteins and their fragments [9]. Here we identified a segment of the SYN involved in the formation of the pathological SYN-TPPP/p25 complex and characterized the functional consequences at molecular and cellular levels using human recombinant wild type and truncated proteins, proteolytic fragments and synthetized peptide as well as CHO10 cell culture.

2. MATERIALS AND METHODS

2.1 Antibodies, peptides

The following antibodies were used: mouse monoclonal SYN antibody against the epitope of 121-125 aa (Sigma, S5566, clone Syn211), rabbit polyclonal SYN antibody developed against the 111-132 peptide sequence in the C-terminal of the protein (Sigma, S3062) or rabbit monoclonal SYN antibody developed against the N-terminal of SYN (Merck, 04-1053, clone EP1646Y); rat polyclonal TPPP/p25 antibody [2]. $SYN^{126-140}$ peptide (EMPSEEGYQDYEPEA) and FITC-labeled peptide (FITC-EMPSEEGYQDYEPEA) were purchased from ChinaPeptides (Shanghai, China).

2.2 DNA manipulations

Prokaryotic expression vector containing the insert for human full length TPPP/p25 was prepared and purified as described previously [12]. The double truncated TPPP/p25 corresponding to amino acid residues 44–174 (TPPP/p25 Δ3-43/Δ175-219) was prepared and purified as described previously [9].

The truncated human SYN corresponding to amino acid residues 1-120 (SYN^{1-120}) was amplified by polymerase chain reaction (PCR) using forward primer 5'-GAAGGAGATATACATATGGATGTATTCATGAAAGGAC-3' and reverse primer 5'-TTCATAAGCAAGCTTTTAAGGATCCACAGGCATATCTTCC-3' and pT7-7 SYN wt [30] as a template. The truncated form was made by replacing the wild type SYN cDNA. After digestion with NdeI and HindIII restriction enzymes, the insert was ligated into pT7-7 vector [31]. The C-terminal human SYN peptide corresponding to amino acid residues 95-140 with a His-tag (SYN^{95-140}) was amplified by PCR using forward primer 5'-CAGCCACTCATATGGTCAAAAAGGACCAGTTGGGC-3' and reverse primer 5'-AGATATCTCGAGGGCTTCAGGTTCGTAGTCTTGATACC-3' and pT7-7 SYN wt as a template. After digestion with NdeI and XhoI restriction enzymes, inserts were ligated into pET21c vector (Novagen).

Structures and sequences of all constructs were verified by restriction mapping and DNA sequencing.

2.3 Expression and purification of the human wild type and truncated TPPP/p25

Human recombinant full length and double truncated TPPP/p25 forms possessing a His-tag were expressed in *E. coli* BL21 (DE3) cells and isolated on HIS-Select™ Cartridge (Sigma-Aldrich) as described previously [2, 32]. Protein

concentrations were determined from the absorbance at 280 nm using an extinction coefficient of 10095 M^{-1} *cm^{-1} and 5625 M^{-1} *cm^{-1} for TPPP/p25 and double truncated TPPP/p25, respectively.

2.4 Expression and purification of the human wild type and truncated SYN

Human recombinant full length and truncated SYN forms were expressed in ampicillin-resistant *E. coli* BL21 DE3 cells. Following transformation, BL21-competent cells were grown in LB in the presence of ampicillin (100 μg/ml). Cells were induced with 1 mM isopropyl β-D-1-thiogalactopyranoside, cultured at 37 °C for 2.5 hours and harvested by centrifugation (20 min, 4 °C, 2000 g).

Human recombinant SYN was isolated as described previously [33]. Briefly, the cell pellet was resuspended in buffer A (20 mM Tris–HCl buffer pH 7.5 containing 1 mM ethylenediaminetetraacetic acid and 50 mM NaCl) with 5 mM 2-mercaptoethanol, 10 μM 4-(2-aminoethyl) benzenesulfonyl fluoride hydrochloride, 1 mM benzamidine, 1 μg/ml pepstatin and 1 μg/ml leupeptin; and lysed by sonication. After centrifugation (25 min, 4 °C, 39000 g), the cell suspension was kept at 90 °C for 10 min, and centrifuged again (25 min, 4 °C, 39000 g). The supernatant was loaded to a DE52 column equilibrated with buffer A. After extensive washing, SYN was eluted with 20 mM Tris–HCl buffer pH 7.5 containing 1 mM ethylenediaminetetraacetic acid and 150 mM NaCl.

SYN^{1-120} was prepared as the full length SYN except that the cell pellet was resuspended in buffer B (20 mM Tris–HCl buffer pH 8.0 containing 1 mM ethylenediaminetetraacetic acid and 10 mM NaCl) and the flow-through fraction was collected during chromatography.

The C-terminal SYN fragment possessing a His-tag (SYN^{95-140}) was isolated on HIS-Select™ Cartridge (Sigma-Aldrich) similarly as described for TPPP/p25 [2, 32].

The proteins were concentrated with a YM 3 Diaflo membrane (Amicon, Danvers, MA), dialyzed overnight in 50 mM NH_4-acetate, lyophilized and stored at -80 °C. The purity of proteins was analyzed by sodium dodecyl sulfate polyacrylamide gel electrophoresis (SDS-PAGE). Protein concentration was calculated from the absorbance at 280 nm using an extinction coefficient of 5960 M^{-1} *cm^{-1}, 2980 M^{-1} *cm^{-1} and 4470 M^{-1} *cm^{-1} for SYN, SYN^{1-120} and the C-terminal SYN^{95-140}, respectively. Extinction coefficients were calculated using ProtParam (http://web.expasy.org/cgi-bin/protparam/protparam).

2.5 Limited proteolysis

SYN at 2 mg/ml was digested with 5 μg/ml trypsin (Sigma-Aldrich) in 40 mM phosphate buffer pH 7.4 at room temperature. The digestion was terminated by 15 μg/ml soybean trypsin inhibitor (Sigma-Aldrich). The samples were analyzed by SDS-PAGE, separated on a Tricine-containing two-layer-gel [34] and stained with Coomassie Brilliant Blue R-250 containing 2-mercaptoethanol.

2.6 Enzyme-linked immunosorbent assay (ELISA)

The plate was coated with 5 μg/ml (50 μl/well) TPPP/p25 or SYN forms in phosphate buffered saline (PBS) as described previously [9, 29]. Briefly, after blocking the wells with bovine serum albumin (BSA), the immobilized proteins were incubated with serial dilutions of SYN/digested SYN/truncated SYN forms or TPPP/p25 followed by the addition of either SYN or TPPP/p25 antibody and the corresponding peroxidase conjugated secondary IgG. The bound antibodies were detected using o-phenylenediamine as substrate. The reaction was stopped after 10 min with 1 M H_2SO_4, and the absorbance was read at 490 nm with an EnSpire Multimode Reader (Perkin

Elmer). The binding constants (Kd) were evaluated from the saturation curves by non-linear curve fitting assuming single binding site hyperbola model using the Origin 8.0 software.

In the case of the competitive ELISA, the TPPP/p25 preincubated for 30 min without or with 1 μM SYN/digested SYN/truncated SYN forms or 50 μM $SYN^{126-140}$ peptide at constant concentration was added to the immobilized SYN. The bound TPPP/p25 was quantified by anti-TPPP/p25 antibody as described above. SYN was digested with trypsin for 60 min.

2.7 8-Anilinonaphthalene-1-sulfonic acid (ANS) fluorescence

The fluorescence measurements were performed in 50 mM Tris buffer, pH 7.5 using a Jobin Yvon Fluoromax-3 spectrofluorometer (Jobin Yvon Horiba, Longiumeau, France) at 25°C. The fluorophore was excited at 380 nm, emission was monitored from 400 to 600 nm as described in [18]. All measurements were done in triplicate. Data were processed using DataMax software. A blank spectrum without protein was recorded before addition of the wild type and double truncated TPPP/p25 forms. The concentration of ANS, TPPP/p25/double truncated TPPP/p25 and $ZnCl_2$ was 50 μM, 2.5 μM and 20 μM, respectively. The concentrations of distinct SYN forms were varied as indicated in the figure legends.

2.8 Affinity chromatography

SYN was immobilized to CNBr-activated Sepharose 4B (Amersham) according to the manufacturer's instructions. The SYN bound to Sepharose was packed into columns. The binding capacity of a column was ~1.5 mg SYN per 1 ml Sepharose (column volume ~ 2 ml). The affinity column was equilibrated with phosphate buffer (10 mM phosphate

buffer pH 7.4 containing 10 mM NaCl). 0.5 mg TPPP/p25 without or with 0.5 mg SYN or SYN^{1-120} in 500 μl was loaded to the column, and the column was washed with phosphate buffer (10 ml, 1 ml fractions). The bound proteins were eluted with phosphate buffer containing 100 mM NaCl (5 ml, 1 ml fractions). After each experiment the column was regenerated using 3 cycles of 0.1 M Na-acetate pH 4.0 buffer containing 0.5 M NaCl and 0.1 M Tris pH 8.0 buffer containing 0.5 M NaCl. The flow-through (unbound) and the eluted (bound) fractions were analyzed by SDS-PAGE.

2.9 Microscale thermophoresis (MST)

Human recombinant TPPP/p25 was labeled with the Monolith NT.115 protein labeling kit (NanoTemper Technologies, Germany) using the amine reactive, red fluorescent dye NT-647 NHS according to the manufacturer's instructions. Labeled protein was separated from the unreacted, free dye by buffer-exchange column chromatography. The labeled TPPP/p25 and the various SYN stock solutions were centrifuged at 17 000 g for 5 min at room temperature prior to the assays. Experiments were carried out in 10 mM phosphate buffer pH 7.4 containing 10 mM NaCl, 0.5 mg/ml BSA and 0.1% Tween-20 with a Monolith NT.115 Microscale Thermophoresis Red/Blue instrument using hydrophobic capillaries (NanoTemper Technologies, Germany). The fluorescence signal was kept above 200 units by modifying the LED power between 20-50%.

The dilution series of the SYN, SYN^{95-140} or $SYN^{120-140}$ yielded 16 different protein concentrations starting from 5-20 μM; the concentration of the labeled TPPP/p25 was kept constant (15 nanoM). After 5 min incubation at room temperature, the samples were loaded into capillaries. Thermophoresis and temperature-jump was measured at 25 °C for 30 sec with 20-50% LED power and 40% MST power, LED color was set to red.

Fluorescence emission was recorded for 5 s before and after the laser was switched on with data collection throughout; while the delay was set to 25 sec. Data were normalized to an arbitrary initial fluorescence value. The MST signal detects the binding based on the change in the normalized fluorescence [35-37].

2.10 Cell Culture and Manipulation

CHO10 cells were cultured in DMEM supplemented with 10% fetal calf serum, 100 units/ml streptomycin and 100 μg/ml penicillin (all reagents from Sigma) in a humidified incubator at 37 °C with 5% CO_2 [11, 12]. For microscopic analysis, cells were grown on 12 mm diameter coverslips. The uptake of the human recombinant TPPP/p25 and/or SYN species were as follows: 3 μl and 12 μl were premixed from 1 mg/ml stock solutions of the full length or double truncated forms of TPPP/p25 and SYN, respectively, then added to 500 μl medium and incubated for 3 hours. The final concentration of the full length species of TPPP/p25 and SYN were 0.24 μM and 1.68 μM, respectively. In the case of FITC labeled peptide, 1 μl of a 10 μg/μl (440 μM) stock was used with the TPPP/p25 forms.

2.11 Immunocytochemistry

After treatment, CHO10 cells were fixed with ice-cold methanol for 10 min, followed by postfixation with 4% formaldehyde (Sigma-252549) for 10 min. After washes with PBS (3x10 min), samples were blocked for 30 min in PBS with 30 μM digitonin containing 5% fetal calf serum. Subsequently, the cells were stained with mouse monoclonal antibody against SYN (epitope of 121-125 aa, Sigma-Aldrich, clone Syn211) or rabbit monoclonal against the N-terminal of SYN (Merck, 04-1053) and polyclonal rat sera against human recombinant TPPP/p25 [2] followed by Alexa 488

conjugated anti-mouse antibody and Alexa 546 conjugated anti-rat antibody (Invitrogen). The samples were washed thrice with PBS for 10 min after antibody incubation. To detect the FITC-labeled peptide, its intrinsic fluorescence was used. Nuclei were counterstained with 4,6-diamidino-2-phenylindole. Images of fixed samples were acquired on a Leica DMLS microscope.

2.12 Statistical analysis

The error bars represent the standard error of the mean (SEM). Comparisons were performed using the unpaired Student's t-test and values were considered to be significant if the calculated P value was <0.05 (*).

3. RESULTS AND DISCUSSION

Recently we have reported that SYN binds to the full length and double truncated (N- and C-terminal free) TPPP/p25 [9]. While the double truncated form displays very low tubulin binding, tubulin polymerization promoting and microtubule bundling activities, its SYN binding and aggregation promoting activity is maintained [9]. The 147-156 aa segment of TPPP/p25 has been suggested to be involved in SYN binding [9].

3.1 Identification of the SYN segment involved in TPPP/p25 binding

In order to obtain information on the segment of SYN involved in the binding of TPPP/p25, trypsin was selected as a protease with its well-defined cleavage specificity. The binding of SYN fragments to TPPP/p25 was tested by ELISA using a specific anti-SYN antibody with an epitope at the C-terminal tail of the protein. A fragment can

display immunopositivity if it contains both the epitope and the TPPP/p25 binding segment. This segment of $SYN^{103-140}$ contains the epitopes of both mono- and polyclonal anti-SYN antibodies as shown in Fig. 1A.

The digestion of SYN with the protease was followed by SDS-PAGE (Fig. 1B); the number and intensity of the peptide bands could be detected in the course of digestions. At 60 min no intact SYN was detected, which could produce false positive result.

Fig. 1C shows the ELISA experiments; in one set of experiments TPPP/p25 was immobilized on the plate, and SYN or digested SYN samples were added in various concentrations; the bound SYN/SYN fragments were detected using anti-SYN antibody developed against the 111-132 peptide sequence in the C-terminus. The mixtures of the SYN fragments obtained by digestion for 60 min displayed immunopositivity, even if it was significantly lower as compared to that of wild type. This finding suggests that there is a tryptic fragment comprising the epitope of the anti-SYN antibody and the binding segment of TPPP/p25.

In another set of experiments the inhibitory potency of the trypsin digested SYN was tested by a competitive ELISA (Fig. 1D). TPPP/p25 premixed without or with SYN/SYN fragments was added to intact SYN immobilized on the ELISA plate; the concentrations of TPPP/p25 were varied in the wells but the concentration of the SYN/SYN fragments was kept constant. The association of TPPP/p25 to the immobilized SYN in the presence of SYN/fragments was detected by an anti-TPPP/p25 antibody. As shown in Fig. 1D, the trypsin digest contains active fragment(s), which can partially inhibit the hetero-association of the two full length proteins in a concentration dependent manner. These data suggest that the binding motive of SYN involved in the interaction with TPPP/p25 is within the 103-140 aa segment of the C-terminal ($SYN^{103-140}$).

3.2 Inhibitory effect of the SYN truncation on the binding of TPPP/p25 to SYN affinity column

Human recombinant SYN mutants as illustrated in Fig. 2 produced by recombinant techniques as described in the Materials and Methods were used to localize the SYN segment within the $SYN^{103-140}$ fragment involved in the binding of TPPP/p25.

In this set of experiments, SYN was immobilized on CNBr-activated Sepharose 4B column as described in the Materials and Methods. The affinity column was equilibrated with 10 mM phosphate buffer, pH 7.4, containing 10 mM NaCl. TPPP/p25 was loaded to the column, which retained the protein according to its capacity (Fig. 3A). When TPPP/p25 premixed with SYN or SYN^{1-120} were loaded to the column, the binding of the TPPP/p25 to the immobilized SYN was highly dependent on the presence of the C-terminal SYN segment (Fig. 3). As illustrated in Fig. 3, the presence of SYN significantly reduced the TPPP/p25 binding due to its powerful competitor capacity. While SYN^{1-120} did not prevent the binding of TPPP/p25, it was still eluted by 100 mM NaCl containing buffer, and the affinity column TPPP/p25 binding capacity was similar to that as in the absence of the competitor SYN. These data indicate the potential role of the 121-140 segment of SYN in the formation of the pathological complex that is stabilized by salt-sensitive electrostatic interactions between the acidic SYN and the basic TPPP/p25. Previously we reported that the binding of TPPP/p25 to its physiological partner, tubulin, is also salt-sensitive; 150 mM NaCl significantly reduced the binding of tubulin to a TPPP/p25 affinity column [38], although their interactions have been proved both in vitro [10, 32] and in different cell lines [9, 11, 39].

3.3 Binding potency of the C-terminal truncated SYN mutants to TPPP/p25

Fig. 4A shows an ELISA experiment in which the binding potency of the truncated forms of SYN was established as compared with that of the full length SYN. SYN species were immobilized on the plate, and then TPPP/p25 was added at different concentrations. Complex formation was detected by a specific polyclonal anti-TPPP/p25 antibody with multiple epitopes [2]. The titration data show that SYN^{95-140} has similar potency as that of SYN to bind to TPPP/p25, while the SYN^{1-120} displays low binding capacity. This finding underlines the role of the 121-140 aa segment in the complex formation.

In another set of experiments, the inhibitory potency of the different truncated SYN forms was analyzed by competitive ELISA (Fig. 4B). TPPP/p25 premixed without or with SYN species at a constant concentration was added to intact SYN immobilized on the ELISA plate, and the effects were detected by an anti-TPPP/p25 antibody similarly as in Fig. 1D. As shown in Fig. 4B, all SYN species with the exception of SYN^{1-120} display significant inhibition on the hetero-association of the two full length protein, which also support that the binding motive of SYN involved in the interaction with TPPP/p25 is within the 121-140 aa segment of the C-terminal.

MST experiments also provided evidence for the role of the unfolded segment of SYN in the pathological interaction with TPPP/p25. MST describes the directed movement of molecules in solution along a temperature gradient depending on the size, charge and solvation shell of molecules [36, 37].

In this set of experiments, TPPP/p25 was fluorescently labeled as described in the Materials and Methods, then it was titrated with the SYN or its truncated mutants. As shown in Fig. 4C, the initial fluorescence values as a function of concentration of SYN or SYN^{95-140} indicate significant binding for both SYN and SYN^{95-140}, but a very low one for the SYN^{1-120}. The fluorescent time traces taken from a representative experiment are

shown (Fig. A1A-A1C). This finding concerns with that suggested by the ELISA data, namely the binding domain of SYN is localized within the 121-140 aa region.

3.4 Effect of SYN on the Zn-induced structural changes of TPPP/p25 sensed by ANS

It has been shown that the interaction of the two disorder proteins, TPPP/p25 and SYN, does not induce structural changes as detected by circular dichroism spectroscopy [22]. ANS is frequently used to identify the molten globule structure, but not the globular or unfolded state of a protein [40, 41]. Previously we have reported that the zinc cation specifically binds to the zinc binding motif of TPPP/p25, $His^{61}(X)_{10}His^{72}(X)_7Cys^{80}(X)_2Cys^{83}$, promoting the formation of a molten globule structure as detected by ANS fluorescent assay [18]. We investigated the effect of the binding of various SYN forms to TPPP/p25 or double truncated TPPP/p25 on the Zn^{2+}-induced molten globule structure.

Fig. 5A and 5B show that upon the addition of ANS to TPPP/p25 the fluorescence intensity increased displaying an emission spectrum with a maximum at 475 nm. The addition of SYN resulted in a small decrease in the fluorescence spectrum of TPPP/p25 with ANS. By adding Zn^{2+} to TPPP/p25 in the presence of ANS, the intensity increased, as expected; however, this effect was completely abolished in the presence of SYN. This effect reached at 2.5 μM SYN concentration is similar to that obtained with the double truncated TPPP/p25 (Fig. 5C-D), in agreement with the previous finding that the core segment of TPPP/p25 is responsible for SYN binding. This sensitive assay was used to test the nature of the interaction of TPPP/p25 species with the SYN fragments (Fig. 5 and A2).

Fig. 5B and D illustrate the results of a series of experiments obtained by ANS assay. The columns symbol the fluorescence emission of the full length (Fig. 5B) and the

double truncated TPPP/p25 (Fig. 5D) measured at 475 nm with the different SYN variants at its saturation values (2.5 μM, except for SYN^{95-140} fragment and the $SYN^{126-140}$ peptide, which are 10 and 100 μM, respectively) in the presence and absence of zinc. It is worth noting that the addition of either SYN forms to ANS does not result in alteration in the fluorescence. The Zn^{2+} is in excess as compared to the SYN excluding the possibility that its metal ion binding accounts for the observed alteration.

All these data suggest that a rather loosely packed hydrophobic core of TPPP/p25 exists in the neighborhood of the zinc finger motif, and the addition of Zn^{2+} promotes a loose molten globule conformation with marginal stability. However, the effect of Zn^{2+} is diminished in the presence of SYN and the fragments (SYN^{95-140} fragment and $SYN^{126-140}$ peptide), which exhibit binding potency to TPPP/p25, prevent the structural rearrangement of the flexible region. In contrast to this, the SYN^{1-120} form does not influence the effect of the bivalent Zn^{2+} cation.

3.5 Intracellular aggregates of the partners: the pathological complex

Previously we have reported that TPPP/p25 and SYN are co-enriched and co-localized in neurons and oligodendrocytes in the cases of Parkinson's disease and MSA, respectively, in spite of the fact that they are expressed alternatively in normal human brain [2, 9]. We also provided evidence for the intracellular co-aggregation, small-size aggregate formation, of the wild type human TPPP/p25 and SYN when these proteins were taken up by CHO10 cells from the medium after premixing [9].

Now we have studied the co-aggregation-prone properties of the full length/double truncated TPPP/p25 and the SYN mutants/fragments/peptide at cellular level in CHO10 cells. The intracellular localization/co-localization of TPPP/p25 and/or SYN were visualized by specific antibodies using red (TPPP/p25) and green (SYN)

fluorescently labeled secondary antibodies as described in details in the Materials and Methods section.

As presented in Fig. 6A and 6B panels, TPPP/p25 or SYN individually is transformed into the cells, the uptake of both proteins is virtually extensive, most of the cells are stained with specific antibodies labeled with fluorescent dyes; however, no aggregation can be visualized. Co-aggregates (small yellow spots by merging the red and green fluorescent labels) are formed when the full length TPPP/p25 premixed with SYN or SYN^{95-140} or FITC-$SYN^{126-140}$ are taken up from the medium by the cells (Fig. 6C, 6E, 6G) indicating the key role of the very C-terminal segment of SYN. No aggregation was observed after the treatment of the cells with the mixture of TPPP/p25 and SYN^{1-120} (data not shown). When the SYN species were co-transported with the double truncated (core) TPPP/p25, a more intensive aggregation was proceeded showing their massive aggregation-prone potency (Fig. 6D, 6F, 6H). This situation does not represent the formation of inclusions such as Lewy body; however, it shows the interactive potency of the segments of the two hallmarks (the core TPPP/p25 and the very C-terminal of SYN) in the constitution of the contact surface of the pathological hetero-complex as well as validates them as a potential drug target.

4. CONCLUSIONS AND BEYOND

NMPs, a subclass of the moonlighting proteins, are frequently major players in neurological disorders by performing functions at both physiological and pathological conditions due to their heteroassociations with distinct partner proteins [8]. TPPP/p25 is a prototype of the NMPs, and it has been defined as a hallmark of synucleinopaties such as SYN [2]. At pathological conditions these two disordered proteins are co-enriched and

co-localized in brain samples characteristic for Parkinson's disease and MSA [2, 42, 43], in spite of the fact, that in normal brain these two hallmark proteins are expressed distinctly in neurons and oligodendrocytes, respectively [13, 23, 24].

We have argued against the targeting of SYN objected by a number of research laboratories to develop anti-Parkinson drugs, since it has multiple functions, in addition, its physiological functions in neurons have not been identified in details [20]. The objective of this work was to present a strategy suitable for the validation of drug targets that is necessary to develop effective agents with unique specificity for therapy by targeting exclusively the pathological complex. As a first step, we identified the interface segment of TPPP/p25 [9] and SYN (in this work) within the TPPP/p25-SYN complex. On one hand, we carried out *in vitro* assays using wild type and mutant human recombinant proteins and fragments, on the other hand, we established a living cell model which renders it possible to visualize the effectivity and the potency of anti-aggregative drugs.

The fact that both HeLa and CHO10 cells can uptake SYN and TPPP/p25 has been recently reported [9]. Endocytosis has been suggested for the mechanism of SYN uptake [44]; and the uptake was found to be concentration-, time-, and clathrin-dependent [45]. The transcellular spread of secreted assembled SYN in human H4 neuroglioma cells by exosomal transmission was demonstrated as well [25]. In addition, the presence of both SYN and TPPP/p25 was detected in the human cerebrospinal fluid [28, 46]. All these data largely contribute to our understanding how TPPP/p25 and SYN can be enriched in inclusions of neurons and oligodendrocytes, respectively, in spite of the fact, that they are expressed alternatively in the two cell types In addition, and they may open the door to a new innovative strategy in anti-Parkinson research. Thus, the message of the present paper is of general scope, namely that proteins with neomorphic moonlighting

functions should not be specific drug targets, rather the interfaces of their pathological complexes.

5. LIST OF ABBREVIATIONS USED

8-Anilinonaphthalene-1-sulfonic acid, ANS; bovine serum albumin, BSA; Enzyme-linked immunosorbent assay, ELISA; microscale thermophoresis, MST; multiple system atrophy, MSA; Neomorphic Moonlighting Protein, NMP; phosphate buffered saline, PBS; polymerase chain reaction, PCR; sodium dodecyl sulfate polyacrylamide gel electrophoresis, SDS-PAGE; α-synuclein, SYN; Tubulin Polymerization Promoting Protein/p25, TPPP/p25;

6. ACKNOWLEDGEMENTS

This work was supported by the European Commission (DCI ALA/19.09.01/10/21526/ 245-297/ALFA 111(2011)29, European Concerted Research Action COST Action TD1406 and TD1304; Hungarian National Scientific Research Fund Grants OTKA T-101039 and T-112144 and Richter Gedeon Nyrt [4700147899] to J. Ovádi.

The funding body had no role in design, collection, analysis and interpretation of data, or in the writing of the manuscript.

7. REFERENCES

[1] G.B. Irvine, O.M. El-Agnaf, G.M. Shankar and D.M. Walsh, Protein aggregation in the brain: the molecular basis for Alzheimer's and Parkinson's diseases, Mol Med 14 (2008) 451-464.

[2] G.G. Kovacs, L. László, J. Kovács, P.H. Jensen, E. Lindersson, G. Botond, T. Molnár, A. Perczel, F. Hudecz, G. Mezo, A. Erdei, L. Tirián, A. Lehotzky, E. Gelpi, H. Budka and J. Ovádi, Natively unfolded tubulin polymerization promoting protein TPPP/p25 is a common marker of alpha-synucleinopathies, Neurobiol Dis 17 (2004) 155-162.

[3] M.G. Spillantini, R.A. Crowther, R. Jakes, M. Hasegawa and M. Goedert, alpha-Synuclein in filamentous inclusions of Lewy bodies from Parkinson's disease and dementia with lewy bodies, Proc Natl Acad Sci U S A 95 (1998) 6469-6473.

[4] A.L. Fink, Natively unfolded proteins, Curr Opin Struct Biol 15 (2005) 35-41.

[5] A.K. Dunker, I. Silman, V.N. Uversky and J.L. Sussman, Function and structure of inherently disordered proteins, Curr Opin Struct Biol 18 (2008) 756-764.

[6] V.N. Uversky, What does it mean to be natively unfolded?, Eur J Biochem 269 (2002) 2-12.

[7] C.J. Jeffery, Moonlighting proteins, Trends Biochem Sci 24 (1999) 8-11.

[8] C.J. Jeffery, Proteins with neomorphic moonlighting functions in disease, IUBMB Life 63 (2011) 489-494.

[9] N. Tőkési, J. Oláh, E. Hlavanda, S. Szunyogh, A. Szabó, F. Babos, A. Magyar, A. Lehotzky, E. Vass and J. Ovádi, Identification of motives mediating alternative functions of the neomorphic moonlighting TPPP/p25, Biochim Biophys Acta 1842 (2014) 547-557.

[10] E. Hlavanda, J. Kovács, J. Oláh, F. Orosz, K.F. Medzihradszky and J. Ovádi, Brain-specific p25 protein binds to tubulin and microtubules and induces aberrant

microtubule assemblies at substoichiometric concentrations, Biochemistry 41 (2002) 8657-8664.

[11] A. Lehotzky, L. Tirián, N. Tőkési, P. Lénárt, B. Szabó, J. Kovács and J. Ovádi, Dynamic targeting of microtubules by TPPP/p25 affects cell survival, J Cell Sci 117 (2004) 6249-6259.

[12] N. Tőkési, A. Lehotzky, I. Horváth, B. Szabó, J. Oláh, P. Lau and J. Ovádi, TPPP/p25 promotes tubulin acetylation by inhibiting histone deacetylase 6, J Biol Chem 285 (2010) 17896-17906.

[13] M. Takahashi, K. Tomizawa, S.C. Fujita, K. Sato, T. Uchida and K. Imahori, A brain-specific protein p25 is localized and associated with oligodendrocytes, neuropil, and fiber-like structures of the CA hippocampal region in the rat brain., J Neurochem 60 (1993) 228-235.

[14] A. Lehotzky, P. Lau, N. Tőkési, N. Muja, L.D. Hudson and J. Ovádi, Tubulin polymerization-promoting protein (TPPP/p25) is critical for oligodendrocyte differentiation, Glia 58 (2010) 157-168.

[15] R.R. Kopito, Aggresomes, inclusion bodies and protein aggregation, Trends Cell Biol 10 (2000) 524-530.

[16] M. Preusser, A. Lehotzky, H. Budka, J. Ovádi and G.G. Kovacs, TPPP/p25 in brain tumours: expression in non-neoplastic oligodendrocytes but not in oligodendroglioma cells, Acta Neuropathol 113 (2007) 213-215.

[17] A. Zotter, A. Bodor, J. Oláh, E. Hlavanda, F. Orosz, A. Perczel and J. Ovádi, Disordered TPPP/p25 binds GTP and displays Mg(2+)-dependent GTPase activity, FEBS Lett 585 (2011) 803-808.

[18] A. Zotter, J. Oláh, E. Hlavanda, A. Bodor, A. Perczel, K. Szigeti, J. Fidy and J. Ovádi, Zn^{2+}-induced rearrangement of the disordered TPPP/p25 affects its microtubule assembly and GTPase activity, Biochemistry 50 (2011) 9568-9578.

[19] J. Oláh, N. Tőkési, A. Lehotzky, F. Orosz and J. Ovádi, Moonlighting microtubule-associated proteins: regulatory functions by day and pathological functions at night, Cytoskeleton (Hoboken) 70 (2013) 677-685.

[20] A. Bellucci, L. Navarria, M. Zaltieri, C. Missale and P. Spano, alpha-Synuclein synaptic pathology and its implications in the development of novel therapeutic approaches to cure Parkinson's disease, Brain Res 1432 (2012) 95-113.

[21] A.A. Valiente-Gabioud, V. Torres-Monserrat, L. Molina-Rubino, A. Binolfi, C. Griesinger and C.O. Fernandez, Structural basis behind the interaction of Zn^{2+} with the protein alpha-synuclein and the Abeta peptide: a comparative analysis, J Inorg Biochem 117 (2012) 334-341.

[22] E. Lindersson, D. Lundvig, C. Petersen, P. Madsen, J.R. Nyengaard, P. Hojrup, T. Moos, D. Otzen, W.P. Gai, P.C. Blumbergs and P.H. Jensen, p25alpha Stimulates alpha-synuclein aggregation and is co-localized with aggregated alpha-synuclein in alpha-synucleinopathies, J Biol Chem 280 (2005) 5703-5715.

[23] L. Maroteaux, J.T. Campanelli and R.H. Scheller, Synuclein: a neuron-specific protein localized to the nucleus and presynaptic nerve terminal, J Neurosci 8 (1988) 2804-2815.

[24] C.A. Bates and W. Zheng, Brain disposition of alpha-Synuclein: roles of brain barrier systems and implications for Parkinson's disease, Fluids Barriers CNS 11 (2014) 17.

[25] K.M. Danzer, L.R. Kranich, W.P. Ruf, O. Cagsal-Getkin, A.R. Winslow, L. Zhu, C.R. Vanderburg and P.J. McLean, Exosomal cell-to-cell transmission of alpha synuclein oligomers, Mol Neurodegener 7 (2012) 42.

[26] S.J. Lee, P. Desplats, H.J. Lee, B. Spencer and E. Masliah, Cell-to-cell transmission of alpha-synuclein aggregates, Methods Mol Biol 849 (2012) 347-359.

[27] K.C. Luk, V. Kehm, J. Carroll, B. Zhang, P. O'Brien, J.Q. Trojanowski and V.M. Lee, Pathological alpha-synuclein transmission initiates Parkinson-like neurodegeneration in nontransgenic mice, Science 338 (2012) 949-953.

[28] O. Vincze, J. Oláh, D. Zádori, P. Klivényi, L. Vécsei and J. Ovádi, A new myelin protein, TPPP/p25, reduced in demyelinated lesions is enriched in cerebrospinal fluid of multiple sclerosis, Biochem Biophys Res Commun 409 (2011) 137-141.

[29] J. Oláh, O. Vincze, D. Virok, D. Simon, Z. Bozso, N. Tőkési, I. Horváth, E. Hlavanda, J. Kovács, A. Magyar, M. Szűcs, F. Orosz, B. Penke and J. Ovádi, Interactions of pathological hallmark proteins: tubulin polymerization promoting protein/p25, beta-amyloid, and alpha-synuclein, J Biol Chem 286 (2011) 34088-34100.

[30] K.E. Paleologou, A.W. Schmid, C.C. Rospigliosi, H.Y. Kim, G.R. Lamberto, R.A. Fredenburg, P.T. Lansbury, Jr., C.O. Fernandez, D. Eliezer, M. Zweckstetter and H.A. Lashuel, Phosphorylation at Ser-129 but not the phosphomimics S129E/D inhibits the fibrillation of alpha-synuclein, J Biol Chem 283 (2008) 16895-16905.

[31] S. Tabor and C.C. Richardson, A bacteriophage T7 RNA polymerase/promoter system for controlled exclusive expression of specific genes, Proc Natl Acad Sci U S A 82 (1985) 1074-1078.

[32] O. Vincze, N. Tőkési, J. Oláh, E. Hlavanda, Á. Zotter, I. Horváth, A. Lehotzky, L. Tirián, K.F. Medzihradszky, J. Kovács, F. Orosz and J. Ovádi, Tubulin polymerization promoting proteins (TPPPs): members of a new family with distinct structures and functions, Biochemistry 45 (2006) 13818-13826.

[33] S.R. Paik, J.H. Lee, D.H. Kim, C.S. Chang and J. Kim, Aluminum-induced structural alterations of the precursor of the non-A beta component of Alzheimer's disease amyloid, Arch Biochem Biophys 344 (1997) 325-334.

[34] H. Schägger and G. von Jagow, Tricine-sodium dodecyl sulfate-polyacrylamide gel electrophoresis for the separation of proteins in the range from 1 to 100 kDa, Anal Biochem 166 (1987) 368-379.

[35] P. Baaske, C.J. Wienken, P. Reineck, S. Duhr and D. Braun, Optical thermophoresis for quantifying the buffer dependence of aptamer binding, Angew Chem Int Ed Engl 49 (2010) 2238-2241.

[36] M. Jerabek-Willemsen, C.J. Wienken, D. Braun, P. Baaske and S. Duhr, Molecular interaction studies using microscale thermophoresis, Assay Drug Dev Technol 9 (2011) 342-353.

[37] S.A. Seidel, P.M. Dijkman, W.A. Lea, G. van den Bogaart, M. Jerabek-Willemsen, A. Lazic, J.S. Joseph, P. Srinivasan, P. Baaske, A. Simeonov, I. Katritch, F.A. Melo, J.E. Ladbury, G. Schreiber, A. Watts, D. Braun and S. Duhr, Microscale thermophoresis quantifies biomolecular interactions under previously challenging conditions, Methods 59 (2013) 301-315.

[38] J. Oláh, N. Tőkési, O. Vincze, I. Horváth, A. Lehotzky, A. Erdei, E. Szájli, K.F. Medzihradszky, F. Orosz, G.G. Kovács and J. Ovádi, Interaction of TPPP/p25 protein with glyceraldehyde-3-phosphate dehydrogenase and their co-localization in Lewy bodies, FEBS Lett 580 (2006) 5807-5814.

[39] L. Tirián, E. Hlavanda, J. Oláh, I. Horváth, F. Orosz, B. Szabó, J. Kovács, J. Szabad and J. Ovádi, TPPP/p25 promotes tubulin assemblies and blocks mitotic spindle formation, Proc Natl Acad Sci U S A 100 (2003) 13976-13981.

[40] G.V. Semisotnov, N.A. Rodionova, O.I. Razgulyaev, V.N. Uversky, A.F. Gripas and R.I. Gilmanshin, Study of the "molten globule" intermediate state in protein folding by a hydrophobic fluorescent probe, Biopolymers 31 (1991) 119-128.

[41] S.S. Leal and C.M. Gomes, Studies of the molten globule state of ferredoxin: structural characterization and implications on protein folding and iron-sulfur center assembly, Proteins 68 (2007) 606-616.

[42] G.K. Wenning, N. Stefanova, K.A. Jellinger, W. Poewe and M.G. Schlossmacher, Multiple system atrophy: A primary oligodendrogliopathy, Ann Neurol 64 (2008) 239-246.

[43] T. Hasegawa, T. Baba, M. Kobayashi, M. Konno, N. Sugeno, A. Kikuchi, Y. Itoyama and A. Takeda, Role of TPPP/p25 on alpha-synuclein-mediated oligodendroglial degeneration and the protective effect of SIRT2 inhibition in a cellular model of multiple system atrophy, Neurochem Int 57 (2010) 857-866.

[44] H.J. Lee, J.E. Suk, E.J. Bae, J.H. Lee, S.R. Paik and S.J. Lee, Assembly-dependent endocytosis and clearance of extracellular alpha-synuclein, Int J Biochem Cell Biol 40 (2008) 1835-1849.

[45] H. Kisos, K. Pukass, T. Ben-Hur, C. Richter-Landsberg and R. Sharon, Increased neuronal alpha-synuclein pathology associates with its accumulation in oligodendrocytes in mice modeling alpha-synucleinopathies, PLoS One 7 (2012) e46817.

[46] R. Borghi, R. Marchese, A. Negro, L. Marinelli, G. Forloni, D. Zaccheo, G. Abbruzzese and M. Tabaton, Full length alpha-synuclein is present in

cerebrospinal fluid from Parkinson's disease and normal subjects, Neurosci Lett 287 (2000) 65-67.

8. FIGURE LEGENDS

Figure 1. Binding of tryptic fragments of SYN to TPPP/p25. (A) Tryptic fragment of SYN containing the epitopes of mouse monoclonal (bold) and rabbit polyclonal (underlined) anti-SYN antibodies. (B) Representative SDS-PAGE image of the time-dependent limited proteolysis of SYN. (C) Binding of the SYN (●) and its fragments obtained by digestion for 60 min (△) to the immobilized TPPP/p25 as detected by polyclonal anti-SYN antibody in ELISA experiment. Error bars represent SEM (n = 3-6). (D) Inhibitory effect of the SYN fragments on the interaction of TPPP/p25 with SYN. TPPP/p25 at different concentrations was preincubated without (white column) or with 1 μM SYN (black column), or its fragments (grey column), and added to the immobilized SYN. The ELISA data were normalized with respect to TPPP/p25 at 0.125 μM without SYN. Error bars represent SEM (n = 3-4).

Figure 2. Characterization of the different SYN mutants. (A) Schematic representation of the various SYN mutants. (B) A representative SDS-PAGE of the SYN mutants. 2 μg protein was loaded to each lane. MM: molecular weight marker. (C) Immunopositivity of the SYN mutants with antibodies of epitopes in the N-terminal (black column) and C-terminal (^{121}DNEAY^{125}, white column) as detected by ELISA experiment. The plate was coated with SYN or its mutant forms, and the interaction was detected by SYN antibodies. Error bars represent SEM (n = 3-5).

Figure 3. Inhibitory effect of the SYN species on the binding of TPPP/p25 to the SYN affinity column. TPPP/p25 was loaded to the SYN affinity column in the absence (A) and in the presence of SYN (B) or SYN^{1-120} (C) following their premixing as described in the Materials and Methods. A-C: Lane 1, molecular weight marker; lane 2-6, unbound fractions; lane 7-11, bound fractions; lane 12, proteins loaded to column.

Figure 4. Effect of the truncation of the SYN on the interaction with TPPP/p25. (A-B) ELISA experiments. (A) TPPP/p25 was added at different concentrations to the immobilized SYN (●, solid line), SYN^{95-140} (◇) or SYN^{1-120} (△, dotted line), and the bound TPPP/p25 was detected by polyclonal TPPP/p25 antibody; and the binding affinities (Kd) are 33.9 ± 5.2 nM and 104 ± 32 nM for SYN and SYN^{1-120}, respectively. Error bars represent SEM (n = 3-9). (B) Competitive ELISA. The plate was coated with SYN, then 0.125 μM TPPP/p25 was preincubated without (white column) or with 1 μM SYN (black column), 1 μM SYN^{1-120} (light grey column), 1 μM SYN^{95-140} (grey column) or 50 μM $SYN^{126-140}$ peptide (dark grey column), and was added to the immobilized SYN. The binding of TPPP/p25 to the different SYN species immobilized on the plate was detected by polyclonal TPPP/p25 antibody. Binding values relative to the control (no SYN) are shown. Error bars represent SEM (n = 3-7). **(C) Microscale thermophoresis.** Binding curves of the various SYN forms to TPPP/p25. The initial fluorescence is plotted as a function of SYN (●), SYN^{95-140} (◇) or SYN^{1-120} (Δ) concentration. A representative experiment is shown.

Figure 5. Effect of SYN species on the molten globule structure of TPPP/p25 detected by ANS fluorescence. Fluorescence spectra of ANS in the absence (dotted line) and presence of SYN (solid line), SYN+Zn^{2+} (short dashed line), TPPP/p25 (dash-dot-

dotted line), TPPP/p25+Zn^{2+} (dashed line), TPPP/p25+SYN (bold line), TPPP/p25+SYN+Zn^{2+} (dash-dotted line). Representative emission spectra are shown. (B) Fluorescence values at 475 nm obtained from similar type of experiments with the truncated SYN species without (black column) or with Zn^{2+} (white column). Error bars represent SEM (n = 3-7). * Significant difference with respect to the ANS and TPPP/p25 without Zn^2. # Significant difference (according to paired Student's t-test, $p<0.05$) between ANS and TPPP/p25 without and with SYN. The concentration of ANS, TPPP/p25, $ZnCl_2$, SYN, SYN^{1-120}, SYN^{95-140} and $SYN^{126-140}$ peptide are 50 μM, 2.5 μM, 20 μM, 2.5 μM, 2.5 μM, 10 μM and 100 μM, respectively. (C, D) Similar set of experiments was carried out with the N- and C-terminal free TPPP/p25. ## Significant difference between the full length and the double truncated TPPP/p25 forms with ANS in absence of Zn^{2+}.

Figure 6. Intracellular aggregates of the heteroassociation of the truncated forms of TPPP/p25 and SYN in CHO10 cells detected by immunofluorescence microscopy. Uptake of the truncated forms of SYN and/or the TPPP/p25 by CHO10 cells from the medium following their premixing as detected by immunofluorescence microscopy. Full length (A, C, E, G) or double truncated (D, F, H) TPPP/p25 and/or SYN (B, C, D), digested SYN fragments (E, F), FITC-$SYN^{126-140}$ (G, H) were taken up by the cells. TPPP/p25 and SYN were immunostained by rat polyclonal TPPP/p25 and mouse monoclonal (epitope ^{121}DNEAY^{125}) SYN antibodies, decorated by fluorescently labeled Alexa546 (red, TPPP/p25) and Alexa488 (green, SYN) secondary antibodies. Note, that the double truncated TPPP/p25 with SYN fragments forms massive aggregates with co-enrichment of the two proteins. The exposure times were 1 s, except in the case of D, F, where it had been reduced to 0.1 s, due to the very high fluorescent intensity of

Figure 1
Click here to download high resolution image

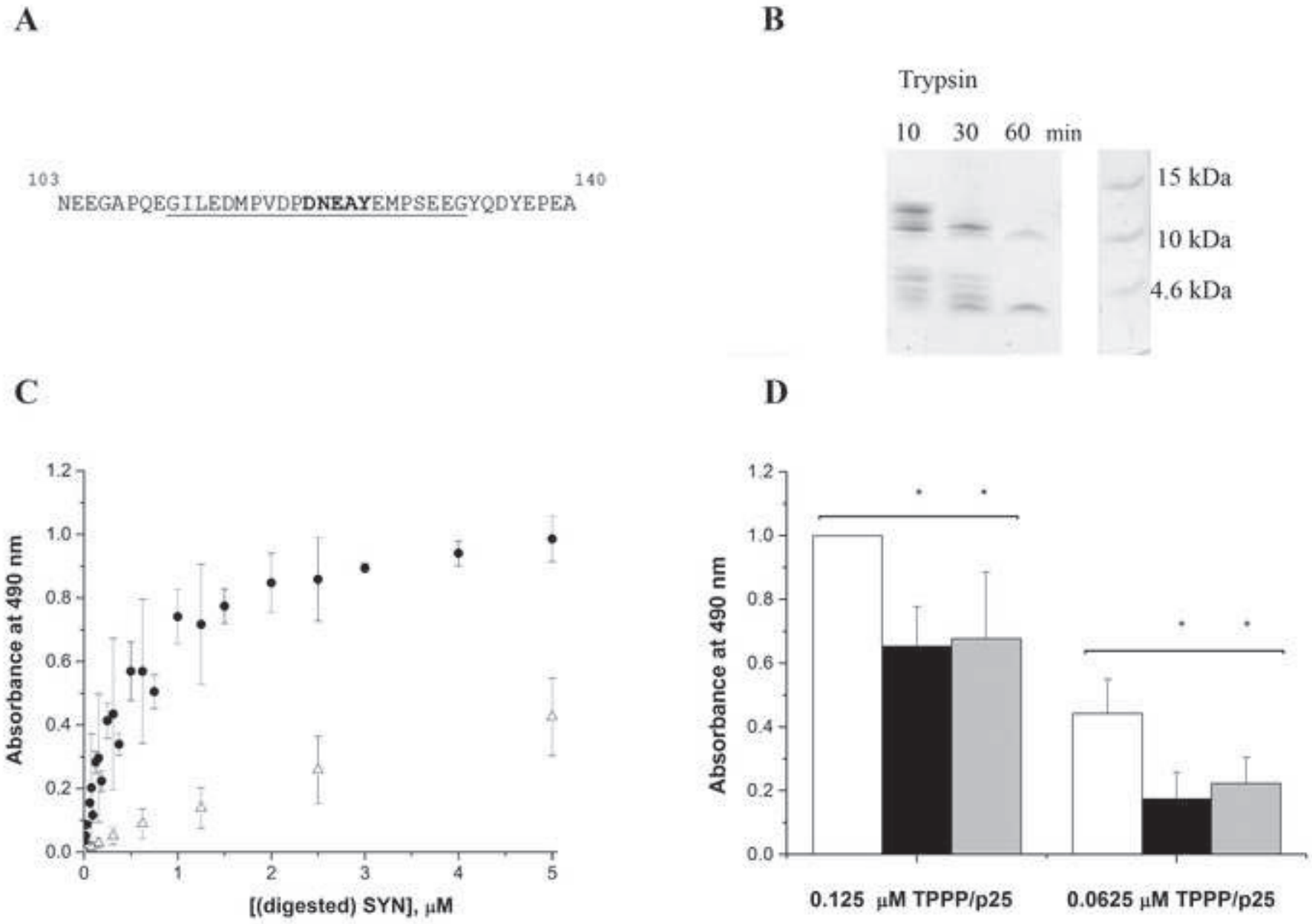

Figure 2
Click here to download high resolution image

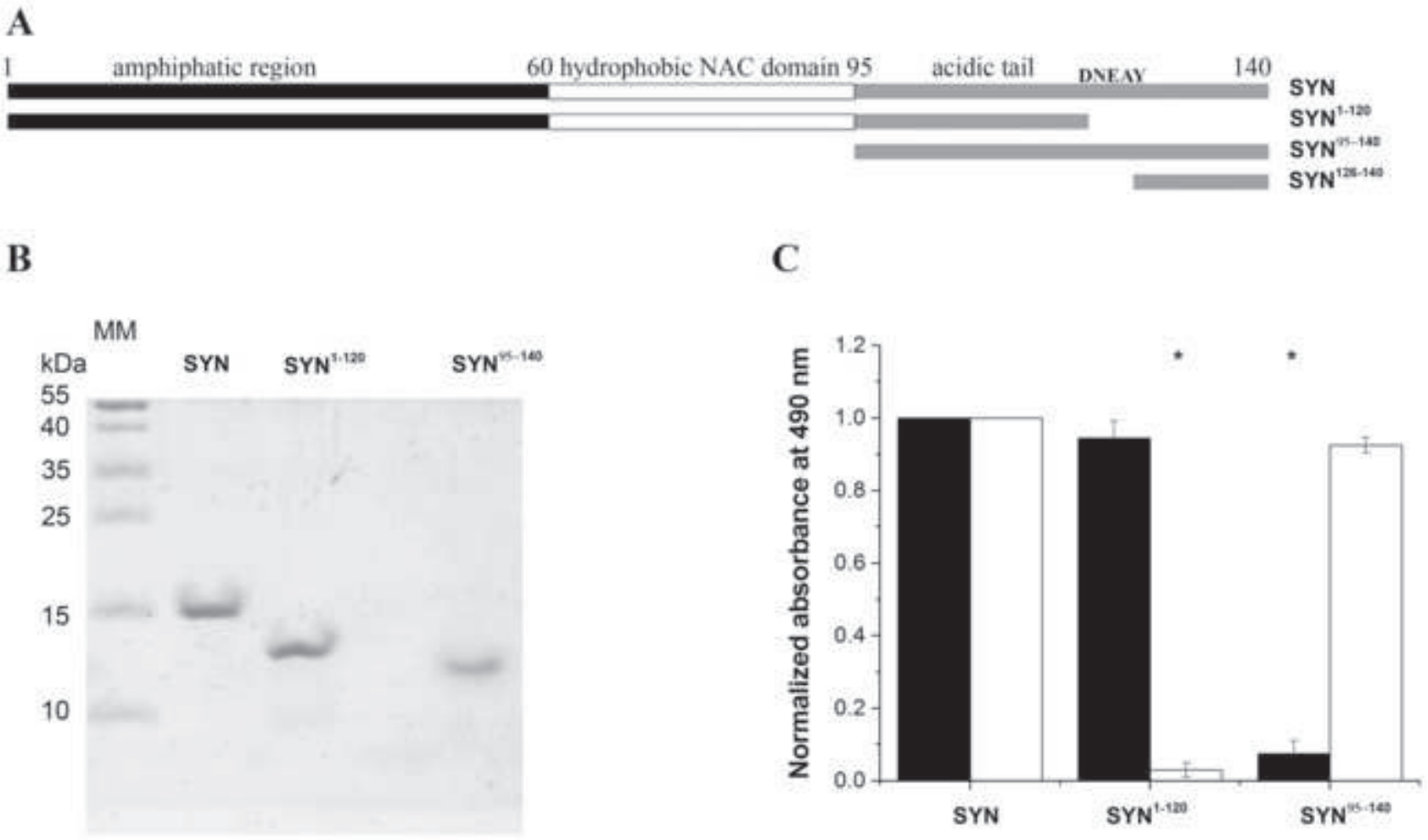

Figure 3
Click here to download high resolution image

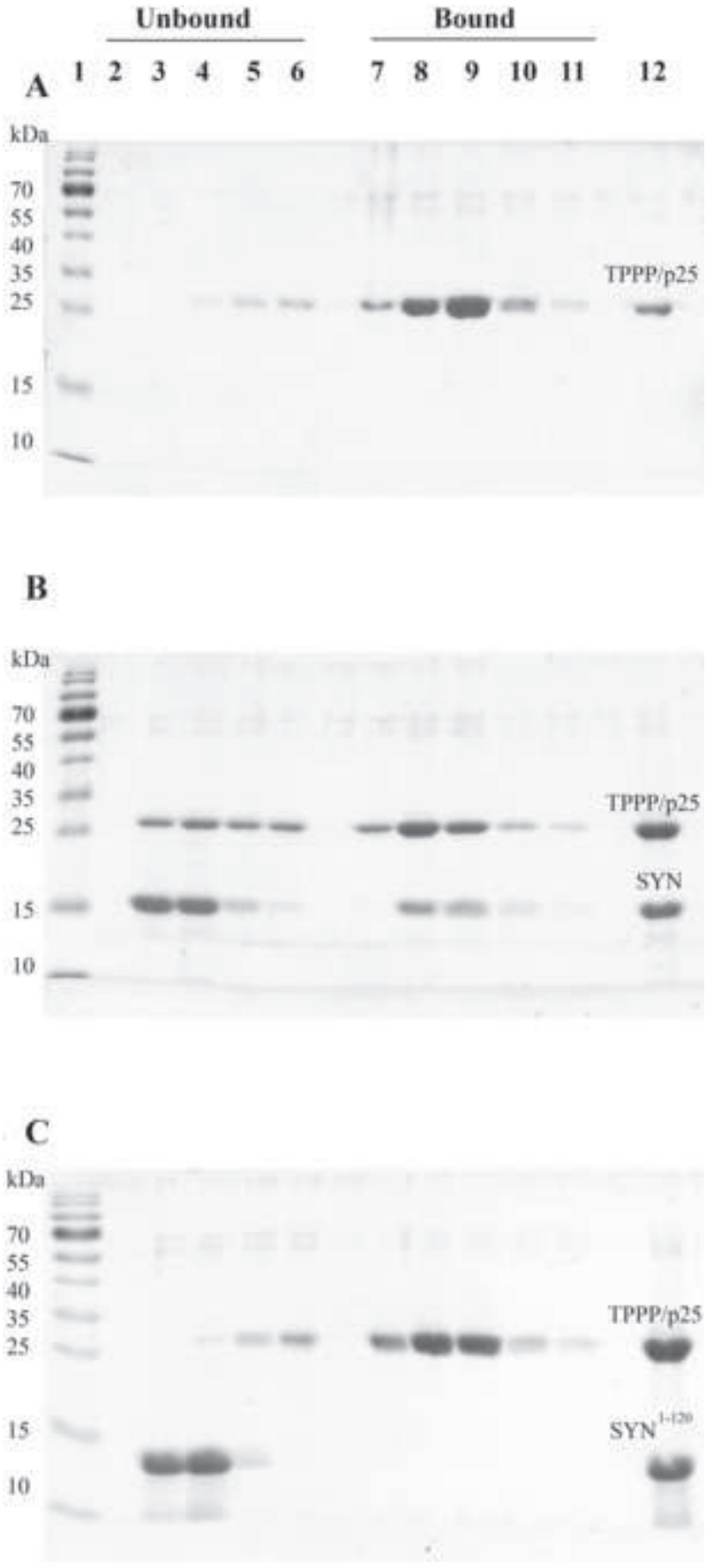

Figure 4
Click here to download high resolution image

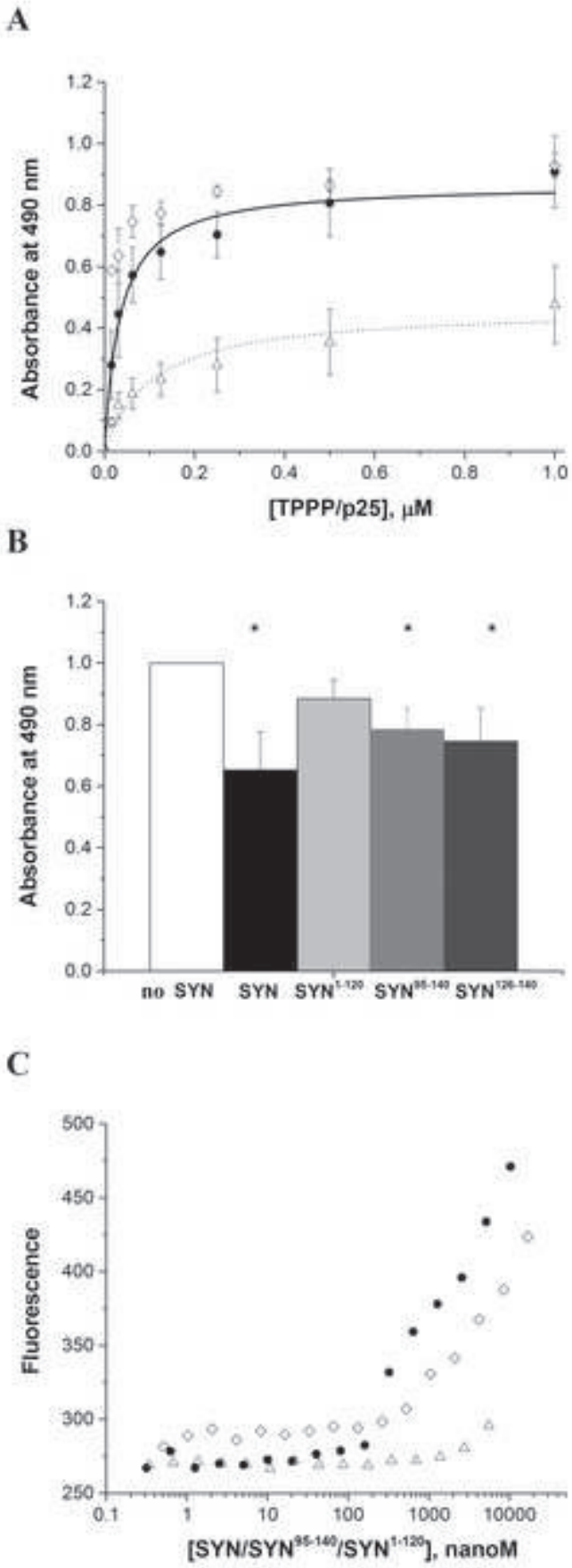

Figure 5

Click here to download high resolution image

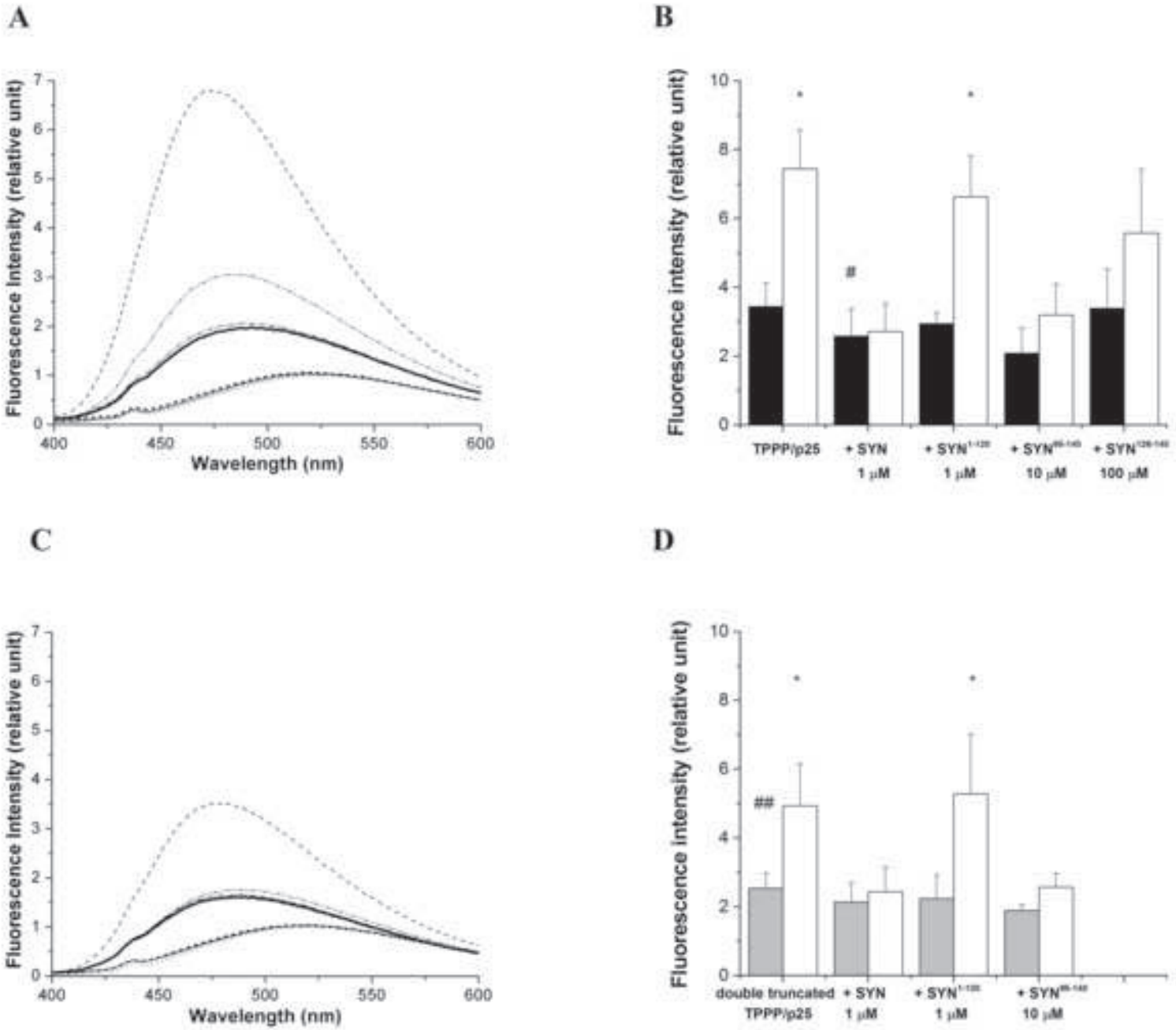

Figure 6
Click here to download high resolution image

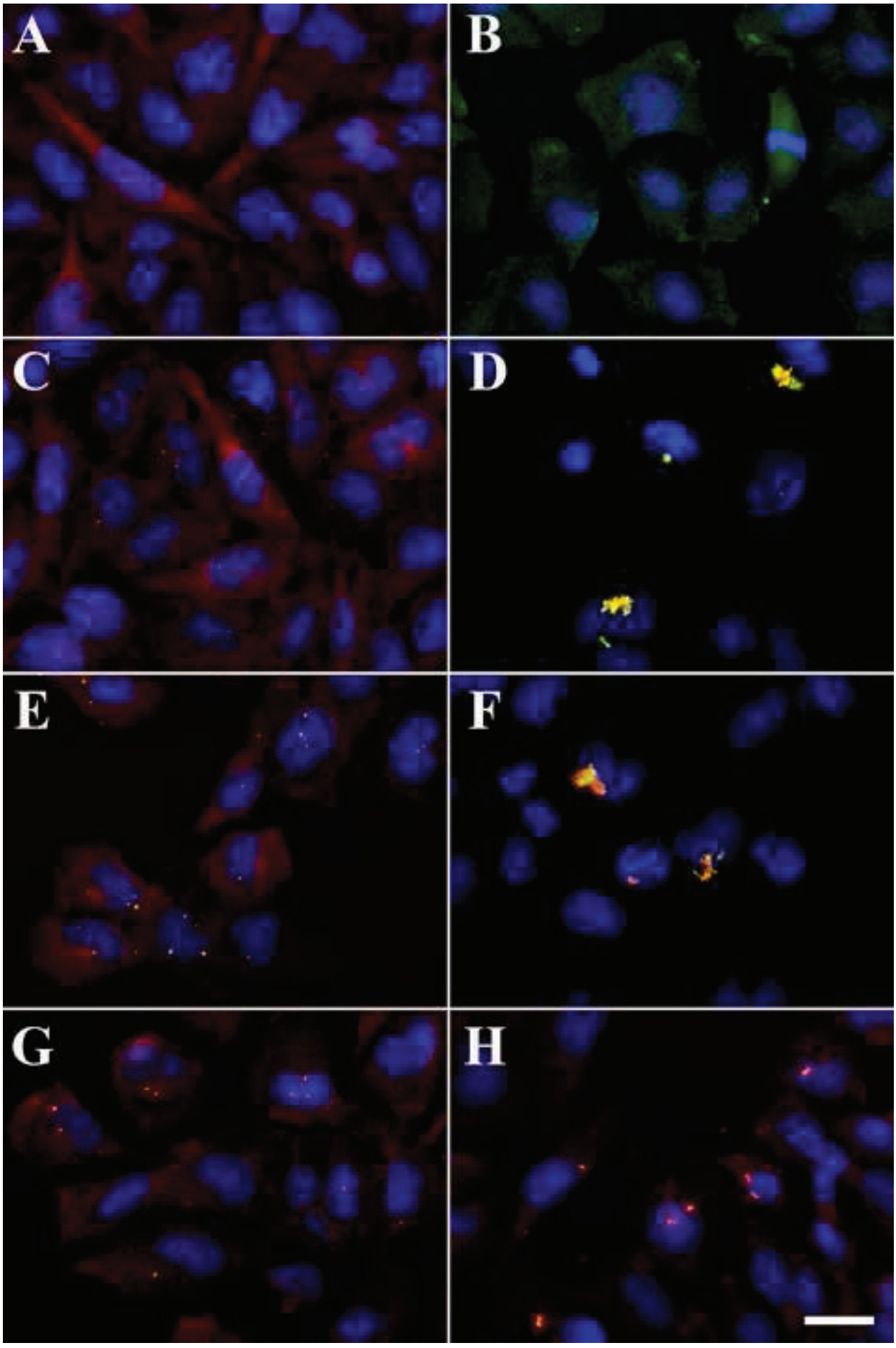

Figure A1. Binding of the various truncated SYN forms to TPPP/p25 by microscale thermophoresis. (A-C) Representative time trace for SYN (A), SYN^{95-140} (B) and SYN^{1-120} (C).

Figure A2. Effect of the various SYN forms on the Zn^{2+}-induced conformational change of the full length (black column) or double truncated (grey column) TPPP/p25 detected by ANS fluorescence. The effect of SYN (A), SYN^{95-140} (B), and $SYN^{126-140}$ peptide (C) as a function of concentration. The concentration of ANS, TPPP/p25/double truncated TPPP/p25 and $ZnCl_2$ was kept at 50 μM, 2.5 μM and 20 μM, respectively. The effects of the various SYN forms are shown in a normalized scale, where the difference of the emission spectra of the full length TPPP/p25 and ANS with and without $ZnCl_2$ at 475 nm equals to 1 unit. Error bars represent the standard error of the determinations (SEM) (n = 3-7). * Significant difference (according to the unpaired Student's t-test, $p<0.05$).

Supplementary Material (for online publication)
Click here to download high resolution image

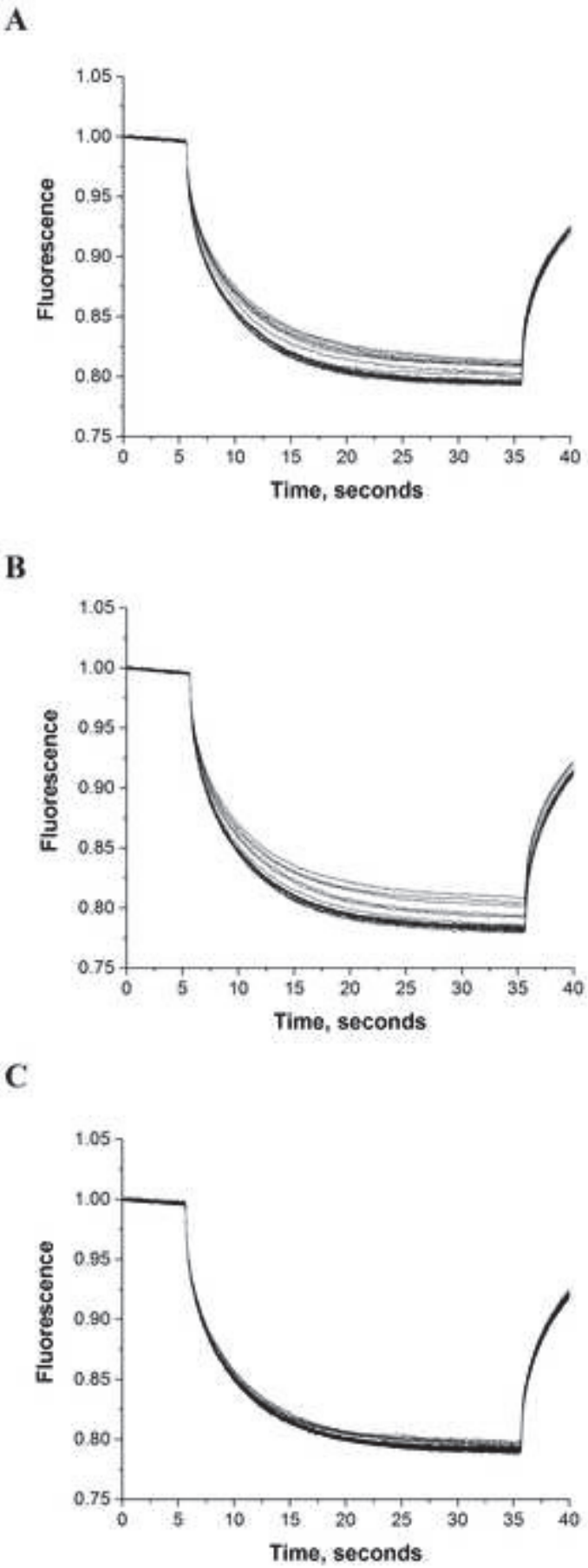

Supplementary Material (for online publication)
Click here to download high resolution image

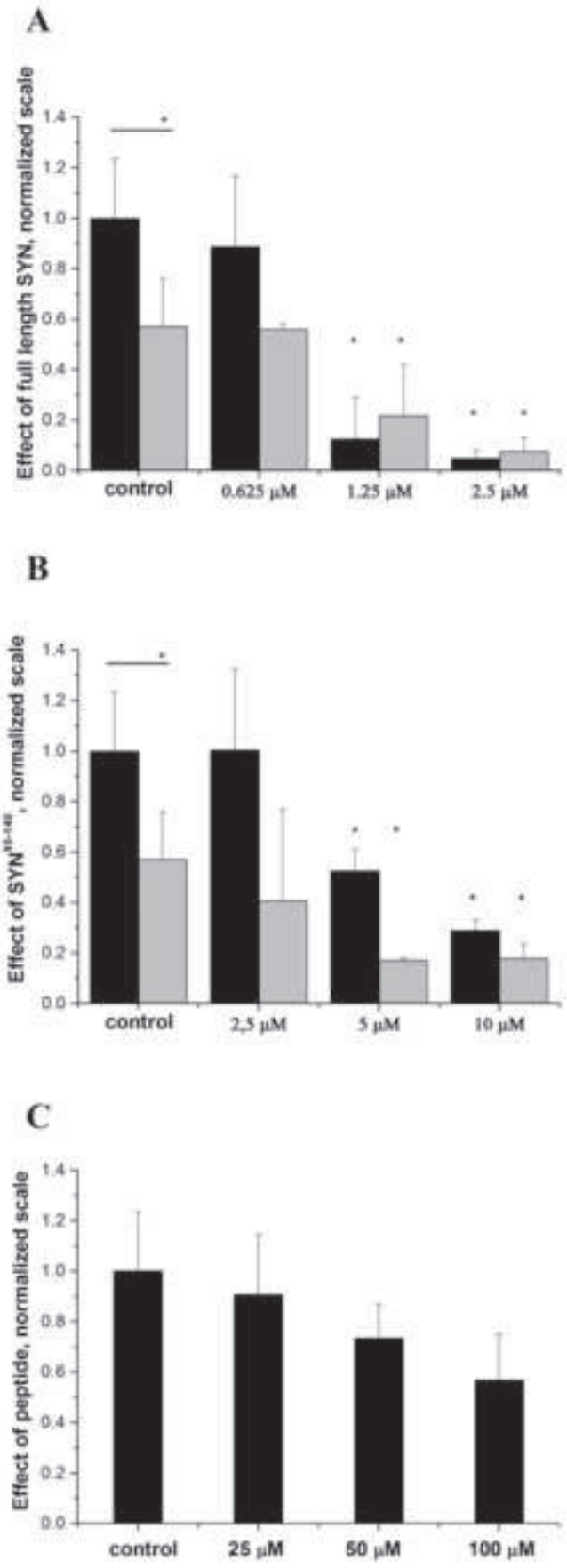

*Conflict of Interest Form

Click here to download Conflict of Interest Form: coi_disclosure_Szunyogh_16092015.pdf

*Conflict of Interest Form

Click here to download Conflict of Interest Form: coi_disclosure_Olah_16092015.pdf

*Conflict of Interest Form

Click here to download Conflict of Interest Form: coi_disclosure_Szenasi_16092015.pdf

*Conflict of Interest Form

Click here to download Conflict of Interest Form: coi_disclosure_Szabo_16092015.pdf

*Conflict of Interest Form

Click here to download Conflict of Interest Form: disclosure_Ovadi_16092015.pdf